AGU100 ADVANCING EARTH AND SPACE SCIENCE

Geophysical Research Letters

RESEARCH LETTER
10.1029/2018GL079773

Key Points:
- The onset of Neoglaciation is regional and driven by nonlinear increases in regional cooling
- Model simulations suggest that cooling onsets are linked to Atlantic Meridional Overturning Circulation
- Observed and simulated rates of late Holocene cooling in the Arctic are remarkably similar

Supporting Information:
- Supporting Information S1
- Table S1

Correspondence to:
N. P. McKay,
Nicholas.McKay@nau.edu

Citation:
McKay, N. P., Kaufman, D. S., Routson, C. C., Erb, M. P., & Zander, P. D. (2018). The onset and rate of Holocene Neoglacial cooling in the Arctic. *Geophysical Research Letters*, *45*. https://doi.org/10.1029/2018GL079773

Received 25 JUL 2018
Accepted 2 NOV 2018
Accepted article online 8 NOV 2018

The Onset and Rate of Holocene Neoglacial Cooling in the Arctic

Nicholas P. McKay[1], Darrell S. Kaufman[1], Cody C. Routson[1], Michael P. Erb[1], and Paul D. Zander[1,2]

[1]School of Earth and Sustainability, Northern Arizona University, Flagstaff, AZ, USA, [2]Institute of Geography and Oeschger Centre for Climate Change Research, University of Bern, Bern, Switzerland

Abstract The middle to late Holocene (8,200 years ago to present) in the Arctic is characterized by cooling temperatures and the regrowth and advance of glaciers. Whether this *Neoglaciation* was a threshold response to linear cooling, or was driven by a regional or Arctic-wide acceleration of cooling, is unknown. Here we examine the largest-yet-compiled multiproxy database of Arctic Holocene temperature change, along with model simulations, to investigate regional and Arctic-wide increases in cooling rate, the synchronicity of Neoglacial onset, and the observed and simulated rates of temperature change. We find little support for an Arctic-wide onset of Neoglacial cooling but do find intervals when regions experienced rapid increases in long-term cooling rate, both in the observations and in climate model simulations. In the model experiments, Neoglacial cooling is associated with indirectly forced millennial-scale variability in meridional heat transport superposed on the long-term decline of summer insolation.

Plain Language Summary Arctic summer temperatures have decreased for the past 8,000 years, before rapidly warming over the past century. As temperatures cooled, glaciers that had melted began to regrow throughout the Arctic, a phenomenon and a time interval known as *Neoglaciation*. This study seeks to understand the nature of this cooling and whether or not this indicates a tipping point in the climate system. Specifically, we use a large database of records from ice cores, lakes, ocean sediment, and more paleoclimate archives to detect patterns of cooling. We investigate these patterns, and climate model simulations, to determine what parts of the Arctic experienced Neoglaciation at the same time, how rapidly it cooled, and what climate models indicate about the causes of cooling. We find that the Arctic did not cool simultaneously, but different regions cooled at different times and that the climate models perform well when simulating both the timing and amount of Arctic cooling.

1. Introduction

By the middle of the twentieth century, an interval of middle to late Holocene glacial advance had been identified in the American Cordilleras and the Arctic (Porter, 2013). Porter and Denton defined *Neoglaciation* as the *the climatic episode characterized by rebirth and/or growth of glaciers following maximum shrinkage during the Hypsithermal interval*. At the time, Neoglaciation was thought to be an asynchronous (and possibly time transgressive) event. Subsequently, Neoglaciation has been identified throughout the Arctic, both through glacial geologic evidence of advance (cf. Matthews, 2013; Solomina et al., 2015) and in continuous records of climatic and glacial variability from lake sediments (e.g., Bakke et al., 2005; Kaplan et al., 2002; McKay & Kaufman, 2009). The middle to late Holocene advance of glaciers in the Northern Hemisphere is an expected response to decreasing summer insolation during the epoch (about 20 W/m^2; supporting information Figure S1; Berger & Loutre, 1991). However, some have suggested (Clegg et al., 2011; Miller et al., 2012, 2017) that Neoglacial cooling was a widespread, nonlinear response of Arctic climate to linear forcing and represents a large-scale *tipping point* in the Arctic system. At the site level, it is difficult to determine whether an observed nonlinear change in temperature or glacier extent was driven by a threshold response in a local system or a tipping point in larger-scale Arctic climate. Additionally, although the spatial structure of the start and end of the Holocene Thermal Maximum (HTM) has been studied in the Arctic using both proxy evidence (Kaufman et al., 2004) and climate models (Renssen et al., 2009), the spatiotemporal pattern of Holocene cooling may not match that of the warming, especially because the pattern of warming was controlled by the size and location of residual ice sheets and the rise of sea level to open channels between the Arctic and Atlantic, neither

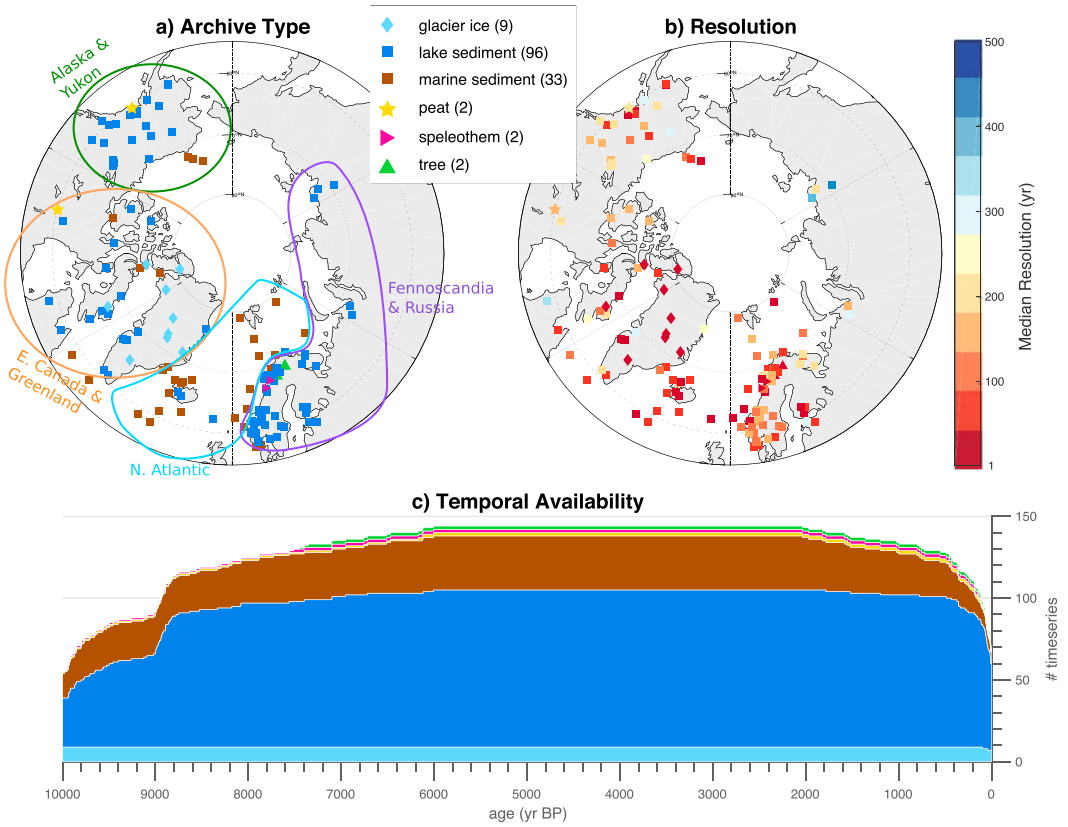

Figure 1. Spatiotemporal paleoclimate data coverage. (a) Geographical distribution by archive type. (b) Temporal resolution determined as the median difference between successive observations. Shapes as in (a), resolution encoded by color. (c) Temporal availability. Colors correspond to archive types in (a).

of which influenced the pattern of cooling following the HTM. Here we examine the spatiotemporal patterns of the onset of Neoglacial cooling, and the rate of cooling, in a large collection of Arctic paleotemperature records. If acceleration of cooling and the regrowth of glaciers were primarily a threshold response to linear summer cooling, the timing would be primarily controlled by local conditions, including elevation, continentality, geomorphology, and the hypsometry of each location, and little regional or Arctic-wide similarity in the timing of the onset is expected. Alternatively, if the onset of Neoglaciation is driven by a regional climate phenomenon, the timing of onset should be regionally coherent and associated with large-scale spatiotemporal patterns. As a further test, we also examine the onset of Neoglacial cooling in climate model simulations, where local threshold effects are minimal and nonlinear responses to forcing are driven by large-scale climate dynamics.

2. Methods

2.1. Arctic Holocene Paleoclimate Data

To examine spatiotemporal patterns of Neoglacial cooling in the Arctic, we use the Arctic Holocene Transitions database version 2.0 (Sundqvist et al., 2014) supplemented by six additional marine sediment records from the North Atlantic described in Sejrup et al. (2016). In total, observations from 144 sites north of 57°N that span at least the interval from 6 to 2 ka with median Holocene temporal resolution of <500 years were included in the analysis (Table S1 and Figure 1). The original studies that describe each reference are cited in Table S1. The Arctic Holocene Transition database is primarily composed of records derived from marine and lacustrine sediments with additional data sets from glacier ice, peat, speleothems, and tree rings. Spatially, the network of observations is densest in Fennoscandia, Alaska and Yukon, and the North Atlantic. Eastern Canada and Greenland are also fairly well represented. Arctic Russia and the Arctic Ocean have little to no data coverage, which reflects the logistical and political challenges of acquiring data from these regions. Of the 144 records used in this analysis, 139 were interpreted by the original authors to represent temperature variability, and five were interpreted to represent the equilibrium-line altitude of glaciers. All of the temperature-sensitive

data sets are used to investigate the timing of Neoglacial cooling, whereas only the 108 records that were quantitatively calibrated to temperature, and thus in units of degrees Celsius, are used to examine the rate of Neoglacial temperature change. Most of the records include some geochronological uncertainty, which could affect both timing and detection of the onset of Neoglaciation. We used Bacon (Blaauw & Christen, 2011) and Banded Age Modeling (Comboul et al., 2014) to create age ensembles for all data sets and propagated these ensembles through all analyses to quantify the impact of age uncertainty (see supporting information).

2.2. Climate Model Simulations

We analyzed model output from the Transient Climate Evolution of the past 21 kyr (TraCE-21) experiments (Liu et al., 2009) to assess potential nonlinear transient responses to low-frequency forcing in the Arctic system. These simulations were conducted with the Community Climate System Model, version 3 (Collins et al., 2006), at T31 resolution (about 3.75° horizontal). In the fully forced experiment, only orbital and greenhouse gas forcings are changing during the mid-Holocene, both of which are approximately linear during the interval. We also investigate changes in orbit, greenhouse gases, meltwater, and ice coverage in single-forcing experiments conducted as part of TraCE-21. Greenhouse gas concentrations were derived from Joos and Spahni (2008), the height and extent of ice sheets was derived from Peltier (2004), and changes in insolation were taken from Berger (1978). The details of the formulation of the meltwater fluxes are described in Liu et al. (2009). In the single-forcing experiments, the geography is held at 21-ka conditions, which means that the Bering Strait remains closed through the Holocene. We also examine two long (1,500- and 3,000-year-long) equilibrium simulations with the same model (Danabasoglu & Gent, 2009).

To examine Holocene temperature change in a greater number of models, we compare mid-Holocene and preindustrial simulations from the Paleoclimate Modeling Intercomparison Project phase 3 (PMIP3; Braconnot et al., 2011; Harrison et al., 2014). These simulations were run with constant forcings at 6 and 0 ka, so they cannot be used to examine the timing of Neoglacial cooling but do offer a perspective on mid-Holocene temperature anomalies across a wide ensemble of general circulation models.

2.3. Detection of the Onset of Neoglacial Cooling

To objectively quantify the timing, and uncertainty, of nonlinear and persistent increases in cooling rate, we developed an iterative algorithm that uses *broken stick* regression (Muggeo, 2003) and searches for the fewest number of significant *breaks* (bends in a piecewise linear regression) that fit the data using only changes in slope that exceed the standard error of the slope of the previous segment. An implementation of this algorithm in R (R Core Team, 2016), which relies on the *segmented* package (Muggeo, 2008), is available as part of the GeoChronR package (McKay et al., 2018). We also quantify the impact of age uncertainty on this result, applying the algorithm across 1,000 age ensemble members derived from either Bacon (Blaauw & Christen, 2011) or Banded Age Modeling (Comboul et al., 2014) age models, resulting in a large output ensemble that quantifies the uncertainty in onset timing due to both regression and geochronological uncertainty. We then aggregate the distributions of *cooling onset* ages (the year in the record, with uncertainty, when cooling rates accelerate) at regional and Arctic-wide scales. This methodology does not impose any a priori constraints on the onset of cooling and can identify cooling that begins before or during what is classically defined as the HTM and may occur earlier than commonly defined as Neoglaciation. However, the detected cooling events are consistent with the definition of Neoglaciation of Porter and Denton (1967). To assess the robustness of the results, we test a null hypothesis by repeating the full procedure on synthetic data that mimic the sample density, chronologic uncertainty, autocorrelation statistics, and first-order trend of the observations (see supporting information).

3. The Onset of Neoglacial Cooling

3.1. Acceleration of Holocene Cooling

The distribution of cooling onset ages and their uncertainties (Figure 2) reveals a complex and regionally variable picture of Holocene cooling in the Arctic. Across all observations (Figure 2a), the area-weighted total distribution of cooling onset ages indicates two primary intervals when cooling began or accelerated. The first, beginning ca. 7 ka primarily captures cooling following peak summer warm conditions in the early to mid-Holocene, when nearly all Arctic glaciers were smaller than during the twentieth century (Figure 3). Importantly, there is little evidence for earlier onsets of cooling, even in regions where peak Holocene warmth occurred early in the Holocene (Kaufman et al., 2004). The second interval, beginning around 2 ka, marks an acceleration of cooling that is most prominent in the North Atlantic and Fennoscandia.

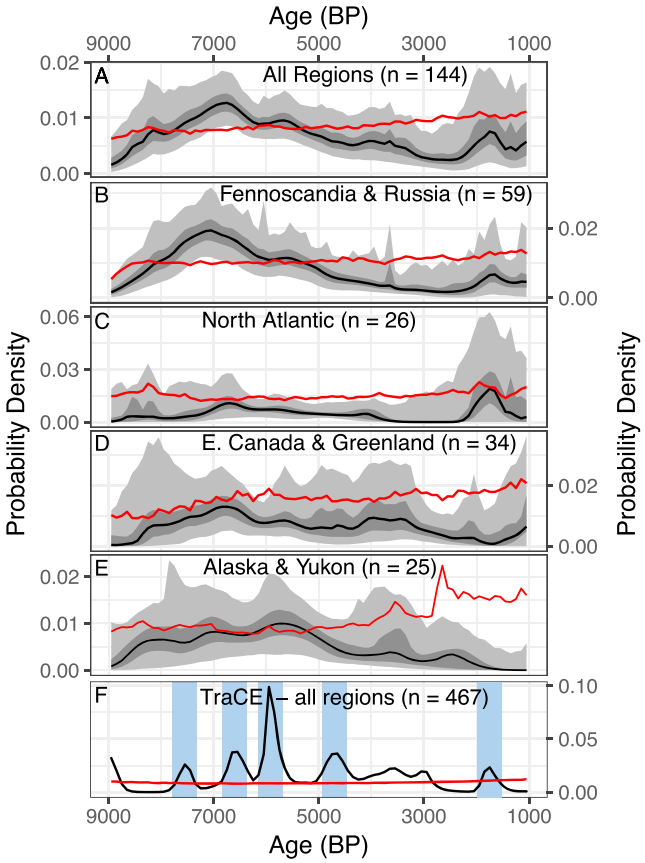

Figure 2. Probability distribution of the timing of the onset of Neoglacial cooling. (a) Area-weighted average onset probability, with uncertainty, for all regions. The 95% and 50% highest density regions incorporating age and broken stick regression uncertainty shown in light and dark gray, respectively. Median probability shown as black line. Red line denotes 95% threshold results from robust null hypothesis testing. (b–e) As in (a) but for each region. Note that the *y* axis varies for each plot and is the largest for panel (c). (f) Onset probability detected in TraCE-21 simulations. Quantiles are not shown in (f) because geochronologic uncertainty does not apply to the model simulations. Blue bars indicate high probability density intervals plotted in supporting information Figure S2.

In addition to our null hypothesis testing, we also assess the consistency of the results when subdividing the database by seasonality (summer compared to annual) and statistical treatment of the data (calibrated compared to noncalibrated; supporting information Figures S5–S8). We find similar results, regardless of how the data are subdivided. Noncalibrated results are noisier and less significant. This may indicate less robust temperature sensitivity of these data, or reflect the impact of smaller sample sizes.

Notably, there is not significant evidence for an onset of Neoglacial cooling occurring at or around 4.2 ka, an interval often implicated for extreme events and Holocene state change (Walker et al., 2012). It has been hypothesized that the *4.2 event* is a hemispheric climate phenomenon that led to prominent glacier advance in much of the Northern Hemisphere (Le Roy et al., 2017). There is some evidence for cooling and glacier advances beginning around this time in Alaska (McKay & Kaufman, 2009), Greenland (Balascio et al., 2015), Iceland (Geirsdóttir et al., 2018), and Norway (Bakke et al., 2010). However, acceleration of cooling ca. 4.2 ka is uncommon, with a notable (but nonsignificant) peak in cooling onset probability around that time found only in Greenland (2d).

The timing of the start of Neoglacial cooling clearly differs among regions. Fennoscandia and Russia (although the data coverage in Russia is limited) are dominated by cooling beginning in the early Holocene (Figure 2b). Some North Atlantic data sets, especially those indicative of annual temperatures (supporting information Figure S7), also show an early Holocene onset of cooling. However, many records in the region are characterized by steady cooling throughout the Holocene until ca. 2 ka, when cooling accelerates in the region (Figure 2c). Eastern Arctic Canada and Greenland show a more variable response without any intervals that

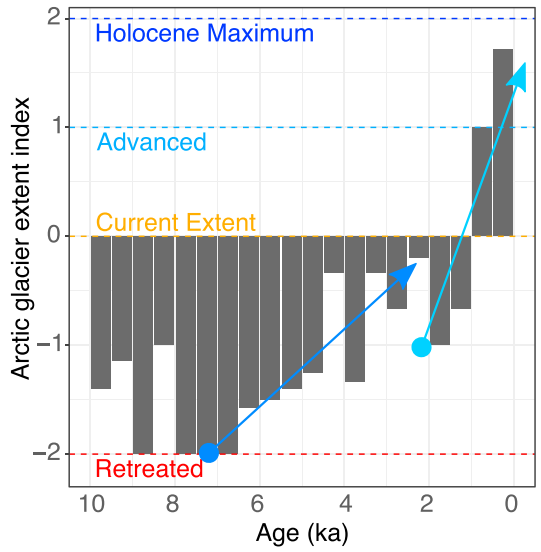

Figure 3. Arctic glacier extent index. Mean qualitative status of Arctic glaciers in 500-year intervals from 10 to 0 ka. Each bar indicates the mean status (averaged over seven regions) for each interval, where 2 = Holocene maximum position, 1 = advanced relative to modern position, 0 = modern position, and −2 = retreated relative to modern position. Arctic glacier status summary is derived from Solomina et al. (2015). Arrows highlight primary intervals of glacier expansion.

appear to be regionally significant (Figure 2d). Alaska and Yukon show a borderline-significant peak ca. 6 ka, an interval that does not appear frequently in other regions (Figure 2e).

The variability in regional timing is consistent with recent regional syntheses of paleoclimate data and other evidence. In Alaska and Yukon, generally warm conditions occurred from 7 to 5 ka, followed by cooling resulting in glacier advances through the late Holocene, with the earliest between 4.5 and 4.0 ka (Kaufman et al., 2016). This aligns with peak cooling onset times in the region between 6 and 5 ka (Figure 2e). In eastern Canada and Greenland, the timing of peak warmth was more variable: more easterly and northerly sites tend to show earlier (ca. 8–7 ka) intervals of maximum warmth, whereas those to the south or west experienced peak warmth ca. 4 ka (Briner et al., 2016). This variability is reflected in the distribution of the timing of Neoglacial cooling onset (Figure 2d), with the highest probabilities following these two warm intervals. The latter interval (ca. 4–3 ka) is also the Holocene minimum extent of the Greenland Ice Sheet, with Neoglacial growth of the ice sheet beginning around this time (Briner et al., 2016). In Fennoscandia, peak Holocene warmth occurred much earlier and more significantly than in the other regions (Sejrup et al., 2016), and Neoglacial began the earliest in this region as well (Figure 2b).

For the most part, the distribution of cooling onset timing is coherent within each region, but the median distributions lie near the 95% threshold of the robust null hypothesis test of our analysis. The variability in the 95% null threshold is driven by the interaction between the density of observations at specific intervals in the data network and the first-order trend present in each time series. The result that there are few intervals of significant change is indicative of both the variability of detected cooling onsets dates in our analysis and the proclivity of autocorrelated data to include sustained changes in trend that are detected by our broken stick regression approach. Nevertheless, the spatial clustering of the probabilities (e.g., the peaks in probability ca. 2 ka in Fennoscandia and the North Atlantic that are absent in western regions) are likely robust features of paleoclimate observations.

3.2. Evidence of Holocene Glacier Expansion in the Arctic

To compare our *cooling onset* results to regional and Arctic-wide intervals of glacier growth, we relied on a recent synthesis of Holocene glacier status (Solomina et al., 2015). Like the pattern of Neoglacial cooling onset (Figure 2), there is considerable variability in changes in glacier status, both within and between regions. Nevertheless, coherent regional and Arctic-wide patterns emerge. Consistent with increases in cooling rate, the large-scale advance of glaciers begins earliest in Scandinavia (ca. 9–7 ka) and most recently in Greenland (ca. 4–3 ka).

To enable larger-scale comparison between Arctic Holocene glacier status and Arctic temperature change, we developed a simple index to quantify and summarize the relative extent of glaciers in the Arctic regions reported in Solomina et al. (2015). The first-order structure of Holocene glaciation in the Arctic is a general increase in the size of glaciers from the early Holocene through the Little Ice Age (Figure 3). From 8–6.5 ka, glaciers were uniformly retreated throughout the Arctic. This is consistent with evidence for warm summer temperatures in Alaska and Yukon (Kaufman et al., 2016), eastern Arctic Canada and Greenland (Briner et al., 2016), the North Atlantic and Fennoscandia (Sejrup et al., 2016), and the northern high latitudes as a whole (Marcott et al., 2013). The widespread warmth during this interval is likely attributable to the combination of high summer insolation in the Arctic (Berger & Loutre, 1991) and the absence of remnant Pleistocene ice sheets that persisted into the early Holocene (Peltier, 2004).

Following this interval of retreat, Arctic glaciers expanded until they reached, on average, near-modern conditions between 4.5 and 2 ka (Figure 3). This represents the first pulse of Holocene Neoglaciation. The second major Neoglacial pulse began ca. 2 ka and culminated during the Little Ice Age when most Arctic glaciers reached their Holocene maximum positions (Solomina et al., 2015). These pulses of Neoglacial advance are consistent with direct evidence of ice expansion from kill dates of entombed plants from Arctic

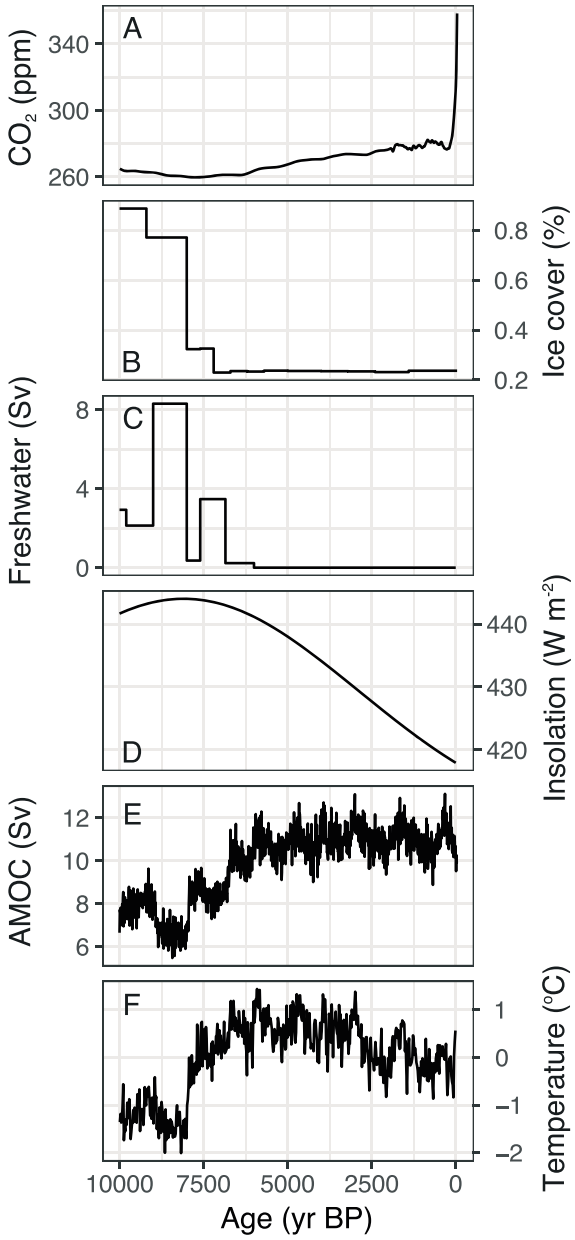

Figure 4. Climate forcings and simulated Arctic temperature and AMOC variability over the past 10 kyr. (a) CO_2 concentration. (b) Fraction of Northern Hemisphere land covered by ice. (c) Northern Hemisphere freshwater forcing. (d) June–August mean insolation at 65°N. (e) Atlantic Meridional Overturning Circulation (maximum MOC in the North Atlantic). And (f) area-weighted mean annual temperature anomaly north of 60°N. Data sources are given in the description of the model setup in section 2. AMOC = Atlantic Meridional Overturning Circulation.

Canada (Miller et al., 2013) and Svalbard (Miller et al., 2017), including the acceleration of advance during the past 2 kyr.

Arctic wide, these two major intervals of Neoglacial onset are consistent with the timing of acceleration of Holocene cooling. Furthermore, we find regional agreement between Neoglacial cooling onset and the expansion of glaciers. This supports the hypothesis that Holocene glacier regrowth is not simply a local threshold effect superposed on gradual cooling but is associated with an increase in cooling rate. However, the cause of these accelerations of cooling cannot be determined from the data alone.

3.3. Acceleration of Cooling in the TraCE-21 Climate Model Simulation

As an additional exploration of the hypothesis that Arctic Neoglaciation was driven by an increase in cooling rates, we apply the broken stick analysis to simulations from the TraCE-21 project (Liu et al., 2009; see section 2). This allows us to assess potential nonlinear transient climate responses to near-linear forcing through the middle to late Holocene. Despite model forcings that only change gradually (Figure 4) and the expected absence of local threshold effects due to the resolution of the model, the fully forced TraCE-21 simulation reveals multiple intervals when the rate of cooling in the Arctic significantly increases. Overall, these *onset events* are more significant relative to the null hypothesis than in the proxy data set (Figure 2f).

The abundance and significance of onset events in the TraCE-21 simulation is an unexpected result. High-frequency climate forcings, including volcanic and solar variability, were not included in the model simulation. Although changes in these forcings very likely influenced the spatiotemporal pattern of real-world Neoglacial cooling, the simulations indicate that nonlinear cooling can occur without high-frequency forcing. The origin of these rapid, indirectly forced, shifts in simulated temperature trends provides insight into how slow changes in forcings and boundary conditions can result in abrupt change in the Arctic. We refer to this variability as *indirectly forced* because the model does not include submillennial-scale forcing during this interval and because unforced control simulations do not exhibit such variability. Arctic-wide mean annual temperature in the simulation (Figure 4) is clearly driven by the combination of ice cover and meltwater forcing in the early Holocene and the gradual decline of summer insolation after ca. 6 ka. Superposed on the long-term trend is pronounced millennial-scale temperature variability, representing about 1 °C of Arctic annual mean temperature variability on ~1,500-year timescales. Examination of the broken stick results indicates that this millennial-scale oscillation is responsible for the change in cooling rates, as in many grid cells the variability superposed on the long-term decline leads to a clear change in trend (supporting information Figure S3).

Changes in the strength of Atlantic Meridional Overturning Circulation (AMOC), and the associated meridional heat transport into the Arctic, explain nearly all of the millennial-scale variability in Arctic temperature and the majority of total variability in the temperature over the past 10 kyr ($R^2 = 0.59$). The cause of this variability in AMOC, however, is unclear, although the amplitude and timescale of variability are consistent with reconstructions of Holocene AMOC variability (Ayache et al., 2018; Ritz et al., 2013; Thornalley et al., 2009). The orbital-only single-forcing experiment shows millennial-scale variability in AMOC, although at a smaller amplitude and shorter timescale than the fully forced simulation. None of the other single-forcing experiments (greenhouse gases, ice sheets, and meltwater forcing) show any evidence of low-frequency AMOC variability. The magnitude and frequency of AMOC variability in the single-forcing experiments are difficult to evaluate because the single-forcing experiments were run with sea level at Last

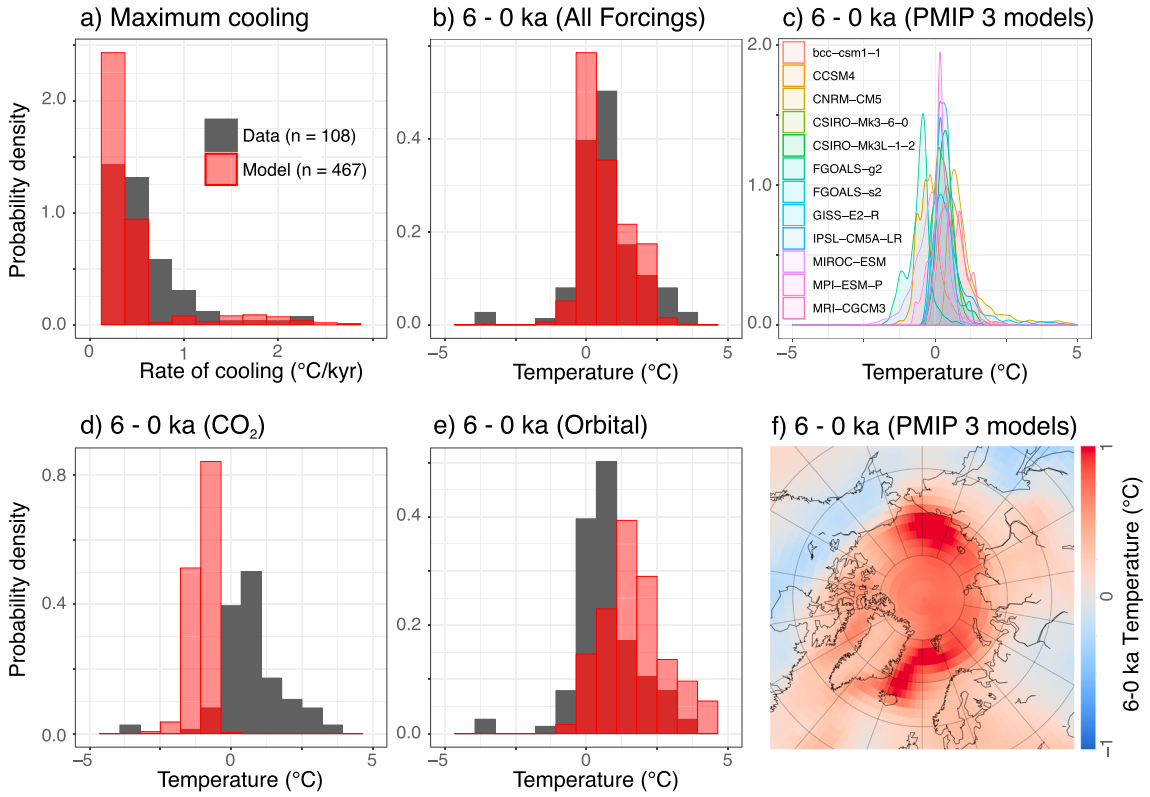

Figure 5. Rate of simulated and observed Arctic Neoglacial temperature change. Simulated temperatures are annual mean surface air temperatures, whereas the proxy data reflect a combination of annual and summer temperature changes (supporting information Table S1). (a) Distribution of cooling rates between warmest and coldest 500-year intervals after 10 ka in each paleoclimate record (dark gray) and model grid cell (red). (b) Distribution of mean simulated and observed temperature differences between the middle (7–6 ka) and late Holocene (1–0 ka) at each site (dark gray) or grid cell (red) for the fully forced TraCE-21 simulation. (c) Distribution of mean near-surface air temperature difference in the 6 ka minus preindustrial simulations from PMIP3. (d, e) As in (b) but for the GHG-only (d) and orbital-only (e) simulations. (f) Composite 6 ka minus preindustrial near-surface air temperature differences in PMIP3 simulations. In (a)–(e), data are presented as probability density to facilitate comparison between the model and data distributions. The data distributions are identical for (b), (d), and (e). Positive differences and rates indicate cooling from 6 to 0 ka. TraCE-21 = Transient Climate Evolution of the past 21 kyr; PMIP = Paleoclimate Modeling Intercomparison Project phase 3; GHG = greenhouse gas.

Glacial Maximum conditions, meaning that the Bering Strait remained closed during the Holocene through these simulations. Long control simulations with the same model and an open Bering Strait do simulate increased variability in AMOC but not at the millennial timescales observed in the fully forced simulation (Danabasoglu & Gent, 2009; supporting information Figure S3). Given the available simulations, orbital forcing seems to be responsible for the simulated variability in AMOC. The mechanism for this is unclear and is the subject of further research.

4. Rate of Neoglacial Cooling

We also compare the rate of temperature change in the Arctic during Neoglacial cooling in paleoclimate observations and climate models. Model simulations for the Holocene disagree with proxy-based temperature reconstructions on the direction of global mean annual temperature trends, a mismatch known as the *Holocene conundrum* (Liu et al., 2014). Recent work suggests that this mismatch, at least in the Northern Hemisphere midlatitudes, may be driven by regional biases (an overemphasis on records from the North Atlantic) and seasonal biases in the proxy data (Marsicek et al., 2018). We find good agreement in the rate and direction of middle to late Holocene temperature trends in the Arctic between model simulations and the paleoclimate data analyzed here.

We calculate Neoglacial temperature changes in two ways, (1) as the rate of change between warmest and subsequent coldest half-millennium since 10 ka at each site and (2) as the simple difference in mean temperature between the middle (7–6 ka) and late (1–0 ka) Holocene. Both approaches reveal strikingly similar rates of Neoglacial temperature change between the data and the model simulations (Figure 5). Most proxy

sites and model grid cells show modest Neoglacial cooling rates, with 84% of the records (90% of the model grid cells) cooling at less than 1 °C/kyr (Figure 5a). Middle to late Holocene temperature differences are comparable and also reveal that, although the majority of sites and grid cells are characterized by cooling, both the data (22%) and the model (19%) have sites that warmed during the late Holocene (Figure 5b). This result is consistent with 12 additional climate model simulations used in PMIP3, indicating that this amount of late Holocene Arctic cooling is a robust feature of both climate models and observations (Figure 5c). Interestingly, in the simulations the most cooling occurred in the Arctic and North Atlantic Oceans (Figure 5f), regions which also experienced significant increases in seasonal sea ice (supporting information Figure S12).

Examining the middle to late Holocene temperature differences simulated in the single-forcing TraCE-21 experiments (Figures 5d and 5e) reveals that cooling simulated in the fully forced experiment is a balance between substantial cooling driven by large decreases in insolation, especially in the summer, and slight warming driven by increases in greenhouse gases. The strong agreement between Holocene temperature reconstructions and model simulations in the Arctic suggests that the implementation of climate processes and feedbacks is simulating realistic climate evolution, at least in this region. These results suggest that the modeled feedbacks, including ice albedo effects in the Arctic, are not significantly biased on long timescales and therefore are not the likely explanation for the Holocene conundrum. The observation that reconstructed and simulated trends are comparable in the Arctic may further implicate the bias in reconstructed seasonality as a major contributor to the Holocene conundrum. Many paleotemperature records are known to be biased toward summer or growing-season conditions (Leduc et al., 2010; Liu et al., 2014). This is also true in the Arctic but may not bias long-term trends in temperature as substantially as at lower latitudes for two reasons. First, increases in summer insolation and temperatures in the Arctic disproportionally impact annual temperatures by controlling glacier and sea ice extent and the expansion of tundra over forest, together which have large impacts on long-term annual mean temperature. This phenomenon is evident in PMIP3 simulations of the mid-Holocene, which consistently show a sustained impact of increased summer insolation on temperature anomalies into the Arctic fall and winter, despite decreases in insolation during these seasons (supporting information Figures S10 and S11). Second, unlike at lower latitudes in the Northern Hemisphere, both summer and annual insolation decrease through the late Holocene due to changes in obliquity, which may mask the impact of summer bias in the proxy data.

5. Conclusions

Our analysis of the largest-yet assembled multiproxy database of Holocene temperature change in the Arctic, paired with examination of climate model simulations, reveals three primary conclusions.

1. There is no evidence for a synchronous, Arctic-wide onset of cooling associated with Neoglaciation. However, within each region there are distinct intervals when the long-term rate of cooling increased. This supports the hypothesis that the onset of Neoglaciation was driven, at least in part, by regional climate dynamics. The regrowth and advance of glaciers in the late Holocene cannot be attributed to site-level threshold effects alone. It is therefore clear that, on Holocene timescales, the Arctic does not behave as a single climatological unit, despite strong forcings.
2. The transient TraCE-21 climate model experiments also simulate nonlinear changes in Arctic temperature in the late Holocene. Cooling onset events in the model are associated with millennial-scale variability in the AMOC, which seems to be associated with orbital forcing, although the precise mechanisms driving this phenomenon in the model remain unclear. It is therefore uncertain to what extent AMOC variability contributed to Arctic Neoglaciation. There is evidence for AMOC and temperature variability on similar timescales during the Holocene (Hoogakker et al., 2011; Risebrobakken et al., 2011; Thornalley et al., 2009). Furthermore, the superposition of millennial-scale variability in meridional heat transport with long-term declines in summer insolation is a plausible explanation for the regional nonlinearity in Holocene temperature trends in the Arctic.
3. Observed and simulated rates of late Holocene cooling in the Arctic are remarkably similar and reflect orbitally driven summer cooling partially offset by greenhouse gas warming during the Holocene.

Acknowledgments
We thank the authors who compiled the Arctic Holocene Transitions data set (Sundqvist et al., 2014) and those who generated and contributed the underlying data (Table S1). This study benefited from three recent regional summaries (Briner et al., 2016; Kaufman et al., 2016; Sejrup et al., 2016) that resulted from the PAGES-endorsed, Arctic Holocene Transitions project. This project was funded by the U.S. National Science Foundation (awards ARC-1107869, EAR-1347213, and AGS-1602105). We also thank two anonymous reviewers for their constructive input to the manuscript. The data used in this study, including the paleotemperature time series, modeled age ensembles, and metadata that describe the climatic interpretation of each record, all encoded as Linked PaleoData (LiPD) files, are available at the World Data Service for Paleoclimatology (https://www.ncdc.noaa.gov/paleo/study/25610), along with the primary outcome of the time series analysis shown in Figure 2.

References

Ayache, M., Swingedouw, D., Mary, Y., Eynaud, F., & Colin, C. (2018). Multi-centennial variability of the AMOC over the Holocene: A new reconstruction based on multiple proxy-derived SST records. *Global and Planetary Change*, *170*, 172–189.

Bakke, J., Dahl, S. O., Paasche, Ø., Riis Simonsen, J., Kvisvik, B., Bakke, K., & Nesje, A. (2010). A complete record of Holocene glacier variability at Austre Okstindbreen, northern Norway: An integrated approach. *Quaternary Science Reviews*, *29*(9-10), 1246–1262.

Bakke, J., Lie, Ø., Nesje, A., & Dahl, S. O. (2005). Utilizing physical sediment variability in glacier-fed lakes for continuous glacier reconstructions during the Holocene, northern Folgefonna, western Norway. *The Holocene*, *15*(2), 161–176.

Balascio, N. L., D'Andrea, W. J., & Bradley, R. S. (2015). Glacier response to North Atlantic climate variability during the Holocene. *Climate of the Past*, *11*, 1587–1598.

Berger, A. (1978). Long-term variations of daily insolation and Quaternary climatic changes. *Journal of the Atmospheric Sciences*, *35*(12), 2362–2367.

Berger, A., & Loutre, M. F. (1991). Insolation values for the climate of the last 10 million years. *Quaternary Science Reviews*, *10*, 297–317.

Blaauw, M., & Christen, J. A. (2011). Flexible paleoclimate age-depth models using an autoregressive gamma process. *Bayesian Analysis*, *6*, 457–474.

Braconnot, P., Harrison, S. P., Otto-Bliesner, B., Abe-Ouchi, A., Jungclaus, J., & Peterschmitt, J. Y. (2011). The Paleoclimate Modeling Intercomparison Project contribution to CMIP5. *CLIVAR Exchanges*, *16*, 15–19.

Briner, J. P., McKay, N. P., Axford, Y., Bennike, O., Bradley, R. S., de Vernal, A., et al. (2016). Holocene climate change in Arctic Canada and Greenland. *Quaternary Science Reviews*, *147*, 340–364.

Clegg, B. F., Kelly, R., Clarke, G. H., Walker, I. R., & Hu, F. S. (2011). Nonlinear response of summer temperature to Holocene insolation forcing in Alaska. *Proceedings of the National Academy of Sciences*, *108*, 19,299–19,304.

Collins, J. A., Bitz, C. M., Blackmon, M. L., Bonan, G. B., Bretherton, C. S., Carton, J. A., et al. (2006). The Community Climate System Model Version 3 (CCSM3). *Journal of Climate*, *19*, 2122–2143.

Comboul, M., Emile-Geay, J., Evans, M. N., Mirnateghi, N., Cobb, K. M., & Thompson, D. M. (2014). A probabilistic model of chronological errors in layer-counted climate proxies: Applications to annually banded coral archives. *Climate of the Past*, *10*(2), 825–841.

Danabasoglu, G., & Gent, P. R. (2009). Equilibrium climate sensitivity: Is it accurate to use a slab ocean model? *Journal of Climate*, *22*, 2494–2499.

Geirsdóttir, Á., Miller, G. H., Andrews, J. T., Harning, D. J., Anderson, L. S., & Thordarson, T. (2018). The onset of Neoglaciation in Iceland and the 4.2 ka event. *Climate of the Past Discussions*. https://doi.org/10.5194/cp-2018-130

Harrison, S. P., Bartlein, P. J., Brewer, S., Prentice, I. C., Boyd, M., Hessler, I., & Willis, K. (2014). Climate model benchmarking with glacial and mid-Holocene climates. *Climate Dynamics*, *43*(3-4), 671–688.

Hoogakker, B. A. A., Chapman, M. R., McCave, I. N., Hillaire-Marcel, C., Ellison, C. R. W., Hall, I. R., & Telford, R. J. (2011). Dynamics of North Atlantic deep water masses during the Holocene. *Paleoceanography*, *26*, PA4214. https://doi.org/10.1029/2011PA002155

Joos, F., & Spahni, R. (2008). Rates of change in natural and anthropogenic radiative forcing over the past 20,000 years. *Proceedings of the National Academy of Sciences*, *105*(5), 1425–1430.

Kaplan, M. R., Wolfe, A. P., & Miller, G. H. (2002). Holocene environmental variability in southern Greenland inferred from lake sediments. *Quaternary Research*, *58*(2), 149–159.

Kaufman, D., Ager, T., Anderson, J., Anderson, P., Andrews, J., Bartlein, P., et al. (2004). Holocene thermal maximum in the western Arctic (0–180°W). *Quaternary Science Reviews*, *23*(5-6), 529–560.

Kaufman, D. S., Axford, Y. L., Henderson, A. C., McKay, N. P., Oswald, W. W., Saenger, C., et al. (2016). Holocene climate changes in eastern Beringia (NW North America)—A systematic review of multi-proxy evidence. *Quaternary Science Reviews*, *147*, 312–339.

Kaufman, D., Schneider, D., McKay, N., Ammann, C., Bradley, R., Briffa, K., et al. (2009). Recent warming reverses long-term Arctic cooling. *Science*, *325*(5945), 1236–1239.

Le Roy, M., Deline, P., Carcaillet, J., Schimmelpfennig, I., & Ermini, M. (2017). ^{10}Be exposure dating of the timing of Neoglacial glacier advances in the Ecrins-Pelvoux massif, southern French Alps, *178*, 118–138.

Leduc, G., Schneider, R., Kim, J. H., & Lohmann, G. (2010). Holocene and Eemian sea surface temperature trends as revealed by alkenone and Mg/Ca paleothermometry. *Quaternary Science Reviews*, *29*(7-8), 989–1004.

Liu, Z., Otto-Bliesner, B., He, F., Brady, E., Tomas, R., Clark, P., & Cheng, J. (2009). Transient simulation of last deglaciation with a new mechanism for Bolling-Allerod warming. *Science*, *325*(5938), 310–314.

Liu, Z., Zhu, J., Rosenthal, Y., Zhang, X., Otto-Bliesner, B., Timmermann, A., et al. (2014). The Holocene temperature conundrum. *Proceedings of the Natational Academy of Sciences*, *111*(34), 3501–3505.

Marcott, S. A., Shakun, J. D., Clark, P. U., & Mix, A. C. (2013). A reconstruction of regional and global temperature for the past 11,300 years. *Science*, *339*, 1198–1201.

Marsicek, J., Shuman, B., Bartlein, P., Shafer, S., & Brewer, S. (2018). Reconciling divergent trends and millennial variations in Holocene temperatures. *Nature*, *554*(7690), 92–96.

Matthews, J. (2013). Neoglaciation in Europe. In S. Elias & C. Mock (Eds.), *Encyclopedia of Quaternary Science* (2nd ed., pp. 257–268). Amsterdam: Elsevier.

McKay, N., Emile-Geay, J., Heiser, C., & Khider, D. (2018). GeoChron development repository. https://doi.org/10.5281/zenodo.60812

McKay, N. P., & Kaufman, D. S. (2009). Holocene climate and glacier variability at Hallet and Greyling Lakes, Chugach Mountains, south-central Alaska. *Journal of Paleolimnology*, *41*(1), 143–159.

Miller, G. H., Geirsdóttir, Á., Zhong, Y., Larsen, D. J., Otto-Bliesner, B. L., Holland, M. M., et al. (2012). Abrupt onset of the Little Ice Age triggered by volcanism and sustained by sea-ice/ocean feedbacks. *Geophysical Research Letters*, *39*, L02708. https://doi.org/10.1029/2011GL050168

Miller, G. H., Landvik, J. Y., Lehman, S. J., & Southon, J. R. (2017). Episodic Neoglacial snowline descent and glacier expansion on Svalbard reconstructed from the ^{14}C ages of ice-entombed plants. *Quaternary Science Reviews*, *155*, 67–78.

Miller, G. H., Lehman, S. J., Refsnider, K. A., Southon, J. R., & Zhong, Y. (2013). Unprecedented recent summer warmth in Arctic Canada. *Geophysical Research Letters*, *40*, 5745–5751. https://doi.org/10.1002/2013GL057188

Muggeo, V. M. (2003). Estimating regression models with unknown break points. *Statistics in Medicine*, *22*(19), 3055–3071.

Muggeo, V. M. (2008). Segmented: An R Package to fit regression models with broken-line relationships. *R News*, *8*(1), 20–25.

Peltier, W. (2004). Global glacial isostasy and the surface of the Ice-Age Earth: The ICE-5G (VM2) model and grace. *Annual Reviews of Earth and Planetary Science*, *32*(1), 111–149.

Porter, S. (2013). Neoglaciation in the American Cordilleras. In S. Elias & C. Mock (Eds.), *Encyclopedia of Quaternary Science* (2nd ed., pp. 269–276). Elsevier.

Porter, S. C., & Denton, G. H. (1967). Chronology of neoglaciation in the North American Cordillera. *American Journal of Science*, *265*(3), 177–210.

R Core Team (2016). R: A language and environment for statistical computing, Vienna, Austria.

Renssen, H., Seppä, H., Heiri, O., Roche, D. M., Goosse, H., & Fichefet, T. (2009). The spatial and temporal complexity of the Holocene thermal maximum. *Nature Geoscience*, *2*, 411–414.

Risebrobakken, B., Dokken, T., Smedsrud, L. H., Andersson, C., Jansen, E., Moros, M., & Ivanova, E. V. (2011). Early Holocene temperature variability in the Nordic Seas: The role of oceanic heat advection versus changes in orbital forcing. *Paleoceanography*, *26*, PA4206. https://doi.org/10.1029/2011PA002117

Ritz, S. P., Stocker, T. F., Grimalt, J. O., Menviel, L., & Timmermann, A. (2013). Estimated strength of the Atlantic overturning circulation during the last deglaciation. *Nature Geoscience*, *6*(3), 208–212.

Sejrup, H. P., Seppä, H., McKay, N. P., Kaufman, D. S., Geirsdóttir, Á., de Vernal, A., & Andrews, J. T. (2016). North Atlantic-Fennoscandian Holocene climate trends and mechanisms. *Quaternary Science Reviews*, *147*, 365–378.

Solomina, O. N., Bradley, R. S., Hodgson, D. A., Ivy-Ochs, S., Jomelli, V., Mackintosh, A. N., et al. (2015). Holocene glacier fluctuations. *Quaternary Science Reviews*, *111*, 9–34.

Sundqvist, H. S., Kaufman, D. S., McKay, N. P., Balascio, N. L., Briner, J. P., Cwynar, L. C., et al. (2014). Arctic Holocene proxy climate database—New approaches to assessing geochronological accuracy and encoding climate variables. *Climate of the Past*, *10*, 1605–1631.

Thornalley, D. J., Elderfield, H., & McCave, I. N. (2009). Holocene oscillations in temperature and salinity of the surface subpolar North Atlantic. *Nature*, *457*(7230), 711–714.

Walker, M. J. C., Berkelhammer, M., Björck, S., Cwynar, L. C., Fisher, D. A., Long, A. J., & Weiss, H. (2012). Formal subdivision of the Holocene series/epoch: A discussion paper by a working group of INTIMATE (Integration of ice-core, marine and terrestrial records) and the subcommission on Quaternary stratigraphy (International Commission on Stratigraphy). *Journal of Quaternary Science*, *27*(7), 649–659.